Environmental and Safety Concerns in Underground Construction, Lee, Yang & Chung (eds)
© 1997 Balkema, Rotterdam, ISBN 90 5410 910 6

A comparison of the Barton-Bandis joint constitutive model with the Mohr-Coulomb model using UDEC

Rajinder Bhasin & Nick Barton
Norwegian Geotechnical Institute (NGI), Oslo, Norway

ABSTRACT: A numerical study is performed to investigate the influence of a joint constitutive model on the stress-strain behaviour of a rock mass. Distinct element simulations are carried out on 3 different block size models of a rock mass using the Barton-Bandis (BB) and the Mohr-Coulomb (MC) joint constitutive models. The results show that the peak shear strength of a rock mass depends on the constitutive law used. The BB model, which allows the modelling of the dilation accompanying shear, predicts results similar to those from reported physical model tests on jointed slabs of a rock model material. A closely jointed rock mass in which block rotations occur exhibits a lower stiffness but a higher strength than a rock mass with widely spaced joints. The MC model, in which the dilation angle is constant, is relatively insensitive to the effects of different block sizes on the stress-strain behaviour of a rock mass.

INTRODUCTION

Numerical models serve as useful tools in simulating the response of discontinuous media subjected to loading. The Discrete Element Method, UDEC [Universal Distinct Element Code, (Cundall (1980), Cundall and Hart (1993)] is a powerful discontinuum modelling approach for simulating the behaviour of jointed rock masses subjected to quasi-static or dynamic loading conditions. In this method, the deformations and volumetric changes of the intact rock material (blocks) as well as the shear and normal displacements along the joints are included.

Due to the high degree of non-linearity of the systems being modelled, explicit (as opposed to implicit) numerical solution techniques are favoured for codes like UDEC (Universal Distinct Element Code). In this technique no matrices are formed as the procedure marches forward in small steps ensuring final equilibrium at each material integration point in the model.

The mechanical behaviour of a jointed rock mass is strongly affected by the behaviour of discontinuities. Therefore, an inevitable component of many numerical techniques is the constitutive model of discontinuities. During the excavation of an underground opening, the jointed rock may slip or separate along the discontinuities and the movement of the rock blocks may occur through translational or rotational shear. A clear understanding of the mechanical behaviour of rock joints is important for analysing and predicting underground structures in jointed rock masses. Several joint constitutive models have been developed in the past two decades for providing a realistic simulation of the mechanical behaviour of rock discontinuities. (*e.g.*, Barton (1982) and Barton and Bandis (1990), Cundall and Hart (1984), Saeb and Amadei (1992), and Souley and Homand (1995). However, it is still customary among many numerical modellers to use the non-realistic linear-elastic Mohr-Coulomb joint constitutive model. This may be attributed to its computational efficiency in numerical codes and the assumed availability of the Mohr-Coulomb parameters for the cohesion intercept and friction angle in the literature.

This paper compares the results from numerical modelling of the stress-strain behaviour of a rock mass using the non-linear Barton-Bandis (BB) joint constitutive model with those from the Mohr-Coulomb (MC) model. The numerical modelling of block size effects and the influence of joint

properties in multiply jointed rock using UDEC-BB has been investigated by Bhasin and Høeg (1997). A brief description of the BB model and some UDEC-BB results are given below:

A BRIEF DESCRIPTION OF THE BB MODEL

The BB non-linear rock joint model describes the shear strength of a joint using the following equation of Barton and Choubey (1977):

$$\tau = \sigma_n \tan\left[\mathrm{JRC}\log\left(\frac{\mathrm{JCS}}{\sigma_n}\right) + \Phi_r\right] \qquad (1)$$

where

σ_n = effective normal stress across the joint

JRC = joint roughness coefficient (0-20) (In Equation 1 the dimension of JRC is in degrees)

JCS = joint wall compressive strength

ϕ_r = residual friction angle

The normal stress (σ_n) versus closure (V_z) relation of a joint in terms of initial normal stiffness K_{ni}, and maximum closure (V_{zm}) is described by Bandis et al. (1981). Their relation for normal stiffness, K_n is as follows:

$$K_n = \left(\frac{K_{ni}}{(1 - V_z/V_{zm})^2}\right) \qquad (2)$$

In the BB model, the secant shear stiffness up to peak (usually called peak shear stiffness) is calculated using the following relationship:

$$K_s = \frac{\tau_p}{\delta_p} \qquad (3)$$

where the peak shear displacement δ_p is given by the following empirical relationship Barton (1990):

$$\delta_p = \frac{L_n}{500}\left(\frac{\mathrm{JRC}_n}{L_n}\right)^{0.33} \qquad (4)$$

where L_n = length of joint in meters and JRC is a coefficient between 0-20 depending on the joint roughness.

The size dependent joint roughness and strength are derived using the following equations proposed by Barton and Bandis (1982):

$$JRC_n = JRC_0\left[\frac{L_n}{L_0}\right]^{-0.02JRC_0} \qquad (5)$$

$$JCS_n = JCS_0\left[\frac{L_n}{L_0}\right]^{-0.03JRC_0} \qquad (6)$$

where the subscripts (0) and (n) refer to the reference joint test length (100 mm) and *in situ* joint length (L_n), respectively.

An appealing feature of the BB-model is that the basic input parameters for rock discontinuities JRC, JCS and ϕ_r are easily measurable in the field or can be obtained through index testing in the laboratory.

NUMERICAL EXPERIMENTS USING UDEC-BB

Table 1 shows the mechanical properties of the intact rock and the BB joint shear strength parameters (JRC, JCS and ϕ_r) adopted for the UDEC-BB modelling studies. The intact rock consists of fully deformable blocks subdivided into finite difference zones to calculate internal stress and strain. These blocks were modelled as linear-elastic and isotropic materials.

Table 1. BB joint parameters and intact rock parameters assumed for the UDEC simulations.

Parameters	Values
Joint roughness coefficient JRC_o	10
Joint compressive strength JCS_o (MPa)	35
Laboratory scale length L_o (m)	0.1
Residual friction angle ϕ_r(°)	25
Uniaxial compression strength σ_c (MPa)	50
Density (ρ) kN/m^3	27.5
Poisson's ratio (υ)	0.25
Deformation modulus E_d (GPa)	20

Distinct element simulations were performed on models of a rock mass of given dimensions but with three different block sizes. The three 1m×1m rock mass models (vertical slabs assumed), shown in Fig. 1, contain two sets of equally spaced persistent joints dipping at an angle of 45° from the horizontal. Joint spacing ranges from 0.3m in model 1 to 0.1m in model 3. For investigating the influence of joint spacing on the stress-strain behaviour of a rock mass, stress boundaries (σ_v=σ_1, σ_h=σ_3) are applied as shown in Fig. 2. As a first step the models were consolidated under the stress $\sigma_1 = \sigma_3 = 2.5$ MPa and from then on σ_1 was increased keeping σ_3 constant.

The strains caused by the deviatoric stresses for the three rock mass models using the BB input data are shown in Fig. 3. For this comparison, the three models had identical input parameters except for the joint spacing. No scaling of the properties was introduced as would be usual in view of the different joint lengths in the three models.

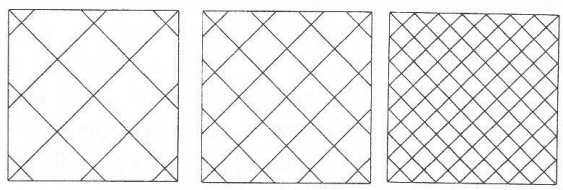

Figure 1. Three discretised assemblies of blocks used for the numerical experiments

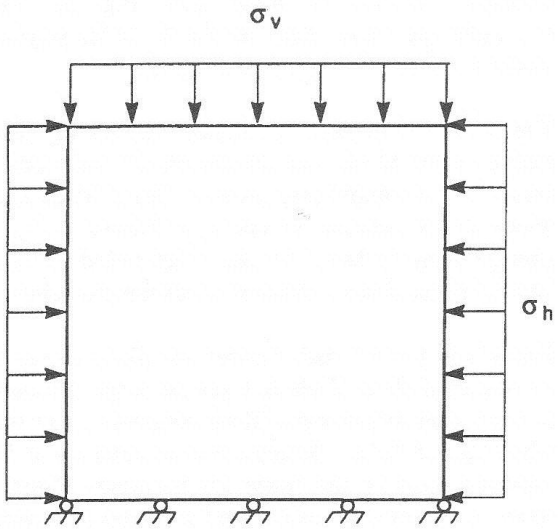

Figure 2. Stress boundary conditions.

The large lateral expansion (mass "Poisson's ratio") is apparent in all the three cases. As block size was reduced, the secant modulus up to a deviatoric stress of 10 MPa reduced from 1.2 to 0.7 GPa (see Fig. 4). At the same level of σ_1 - σ_3, the axial strain in model 1 was smaller than in models 2 and 3. However, a higher deviatoric stress is required to fail model 3 than the two others. The results indicate that the shear strength of a closely jointed rock mass is significantly higher than for a rock mass with wider spacing.

Models 1 and 2 failed as shown in Fig. 5, which presents a displacement vector plot visualising the shear failure for model 1. The contrasting stress-strain behaviour exhibited by the three different models indicates some block size effects on the mass "Poisson's ratio". The ratio of lateral strain/axial strain increases to well beyond = 0.5 as shear strength is increasingly mobilised (see Fig. 3). The

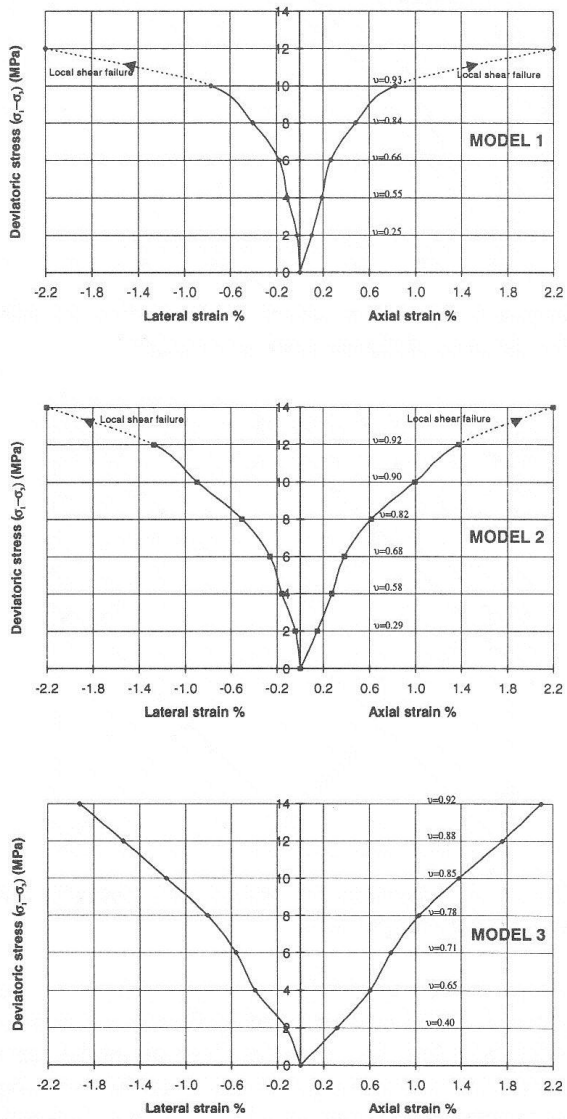

Figure 3. Deformation behaviour exhibited by the three models of different sized blocks.

larger size block assemblies (models 1 and 2) deform mainly through translational shear resulting in a rapid increase in mass "Poisson's ratio" to about 0.92 before the onset of shear failure. At a deviatoric stress of about 8 MPa the mass "Poisson's ratio" in model 3 falls below that of models 1 and 2. At a

deviatoric stress of about 14 MPa the mass Poisson's ratio for model 3 is 0.92. Note that at this stress level models 1 and 2 would probably have had a mass "Poisson's ratio" beyond 1.0, but they failed before that level was reached.

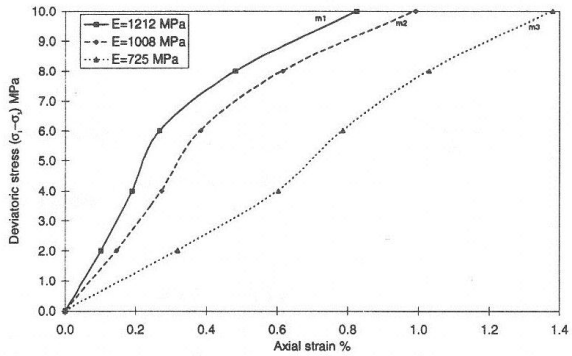

Figure 4 Equivalent secant modulus upto 10 MPa for the three different block size models

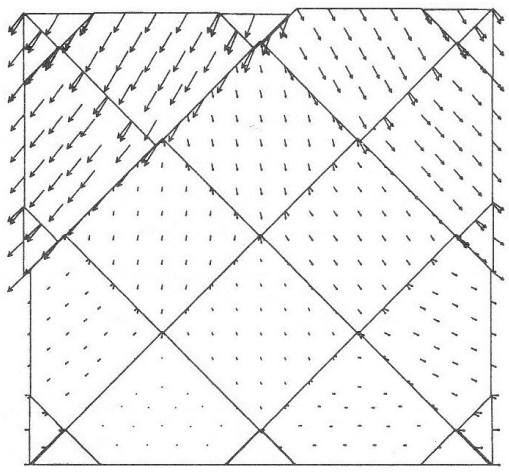

Figure 5. Displacement vector plot showing the shear failure for model 1.

These numerical results are very similar to the physical model tests reported by Barton and Bandis, 1982 (see Fig. 6). In these physical model tests, jointed slabs simulating different cross joint spacing were stressed to failure in a biaxial frame. A double bladed "guillotine" was used for generating model tension fractures (joint sets) through slabs of the weak brittle material, which was formed from an oven-cured combination of red lead-sand-ballotini-plaster-water. The peak strength (τ) of the joints were described closely by Equation (1). The large increase in mass "Poisson's ratio" due to joint shear in the numerical experiments (see Fig. 3) have also been observed in the physical model studies reported by Barton and Hansteen (1979) and Barton and Bandis (1982), and will depend on the orientation of the joints.

The distinctly convex load-deformation behaviour shown by models 1 and 2 in Fig. 4 are typical of a rock mass with diagonal joints. As illustrated schematically in Fig. 7, the shear components are largely responsible for the deformation of a rock mass with diagonal joints. Horizontal joints such as those parallel to the bedding are mainly subjected to normal closure and show a concave load-deformation behaviour. In this case the lateral expansion is limited, and the shear components are largely absent. It is interesting to note that model 3 shows a linear type of load-deformation behaviour due to the combined effect of shearing and closure on an increased number of joints (see Fig. 3). This resembles the axial strain results from the physical model test on 4000 blocks (see Fig. 6).

The present numerical simulations are clearly illustrative of the block size effects on the deformation behaviour of jointed rock masses. Small block sizes which allow rotation to occur, exhibited a higher strength than the larger blocks which failed by translational shear along a number of continuous joints.

Tunnels in jointed rock masses are likely to fail by translational shear if block sizes are large compared to the tunnel dimensions. Block rotations occur only when partial failure through translational shear has occurred creating the space for rotations. Figure 8 shows a special case of failure for model 3 in which a tunnel was excavated at a deviatoric stress of 14 MPa. The increased degree of freedom of the individual joint blocks is apparent from this figure. However kink band development as observed in a 4000 block model [see Fig. 6 and Barton and Bandis (1982)] did not develop in the present 144 block numerical model.

ESTIMATION OF EQUIVALENT c AND ϕ VALUES FROM THE BB JOINT PARAMETERS

In the following, the Mohr-Coulomb parameters c and ϕ are derived from the BB parameters to have consistent comparison. These are then introduced in the 3 models so that the effect of linear joint properties on the predicted behaviour of the rock mass can be investigated. In the BB-model the dilation along the joint develops gradually with shear

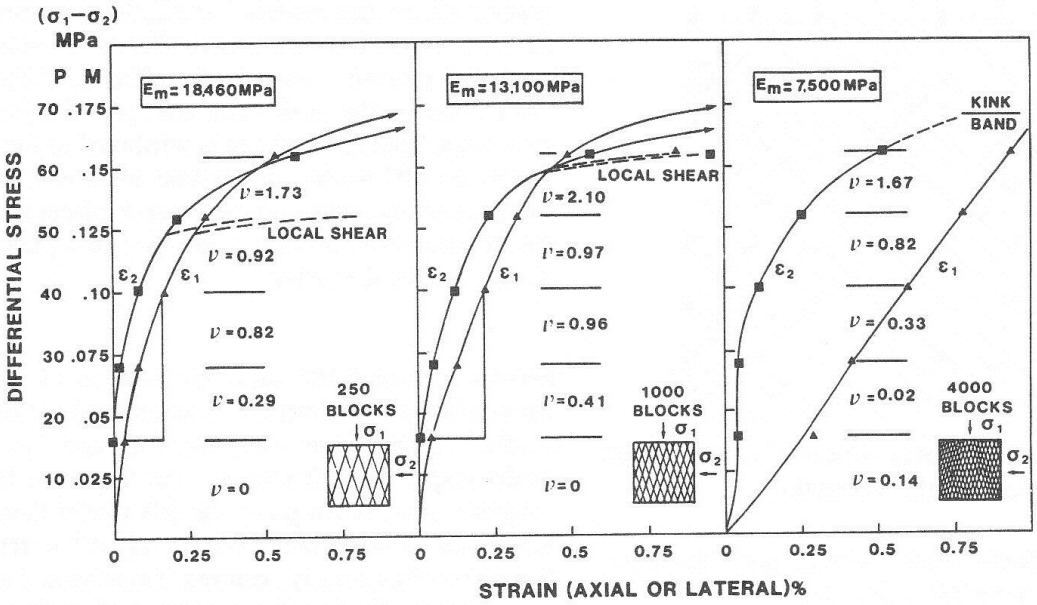

Figure 6 Stress-strain behaviour exhibited by assemblies of different sized blocks, Barton and Bandis ,1982.

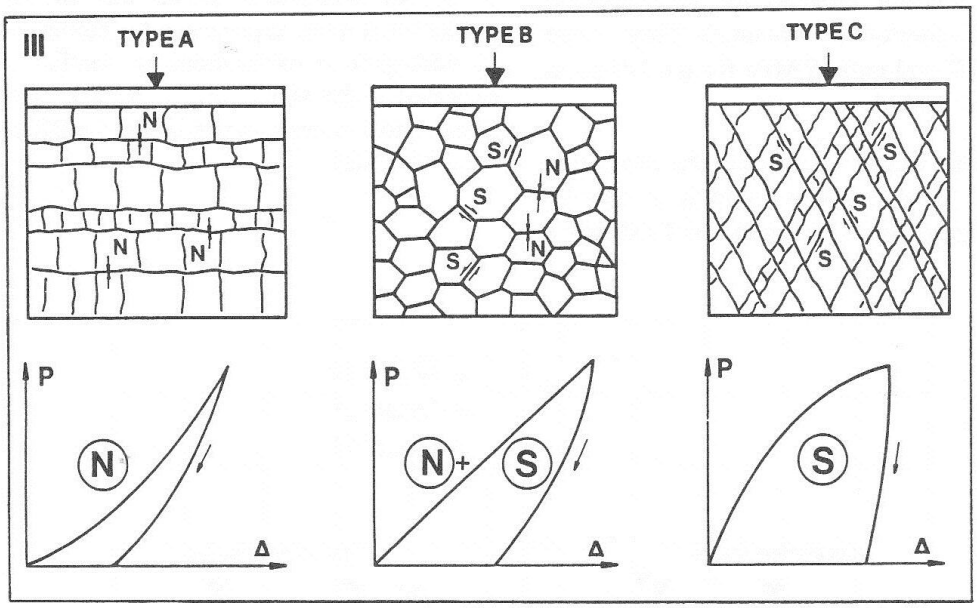

Figure 7 Contrasting load-deformation behaviour for rock masses with different magnitudes of joint shear (S) and normal deformation (N) components, Barton, 1990.

displacement (using the JRC mobilised concept of Barton (1982), and the peak dilation angle is estimated from the following equation:

$$\phi_d = 0.5JRC_n \log\left(\frac{JCS}{\sigma_n}\right) \qquad (7)$$

In the Mohr-Coulomb model, the dilation angle is constant and represents an average value. Therefore a reduction factor of ½ is applied to the above expression to calculate ϕ_d for the Mohr-Coulomb model.

Inside the range of normal stresses relevant (5 and 10 MPa,), we can find the shear strength (τ) based on the BB formulae presented in Equation (1). To be equivalent to the BB-model in the same stress range,

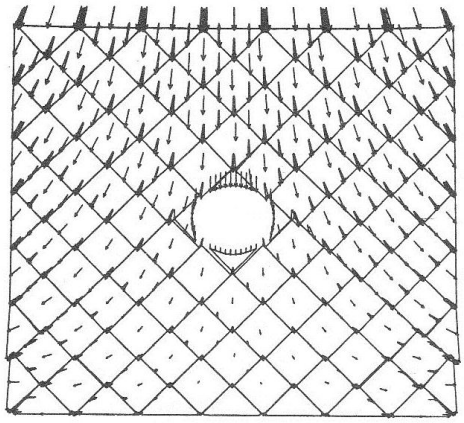

Figure 8 Magnified (×3) visualisation of block movements in model 3 after tunnelling

the Mohr-Coulomb model should give the same shear strength as the BB-model, *i.e.*,

$$\tau_5 = \sigma_n \tan\phi + c \quad (\sigma_n = 5\text{MPa}) \qquad (8)$$

$$\tau_{10} = \sigma_n \tan\phi + c \quad (\sigma_n = 10\text{MPa}) \qquad (9)$$

By solving the above system of equations, the friction angle and cohesion intercept for the equivalent Mohr-Coulomb criterion are obtained. They turned out to be ϕ=24.8° and c=0.45 MPa for the BB-parameters shown in Table 1.

Fig. 9 shows the strains caused by the deviatoric stresses for the three rock mass models. It may be seen from the figure that although model 3 exhibits a lower stiffness than models 1 and 2, the three models fail at the same deviatoric stress. The results indicate a relative insensitiveness to the effect of different block sizes on the peak shear strength of a jointed rock mass. This insensitivity is attributed to the fact that in the MC model, the dilation angle is constant and does not increase with the shear displacement. In the BB model the dilation angle rises to a peak and slowly reduces thereafter.

Figures 10 a and 10b show the rotation of blocks (shown in the figure through rotation arcs) for model 3 after consolidation using the BB and the MC model respectively. It may be seen that more block rotations occur when using the BB model than the MC model. Block rotation occurs only when translational shear has already occurred. Translational shear in fact causes dilation of the joints creating the space for rotations. It is widely acknowledged that the degree to which a rock joint dilates when sheared has important consequences in rock mechanics. Thus, for non-planar joints the BB-model may render itself more appropriate for numerical analyses of underground excavations if dilation effects are expected to be significant. However, the computational effort is larger when using the BB-model than the MC model.

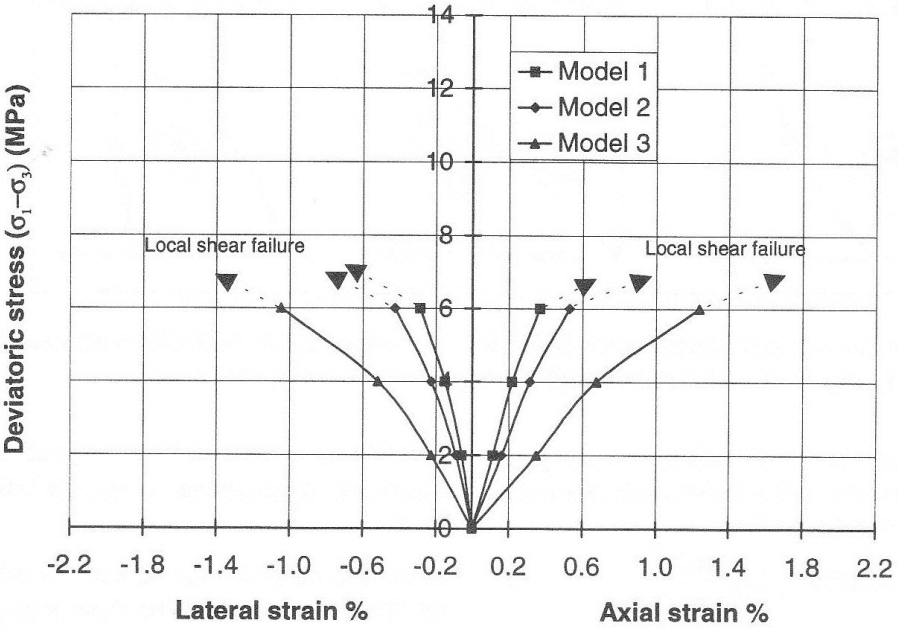

Figure 9 Deformation behaviour exhibited by the three models when using the MC model

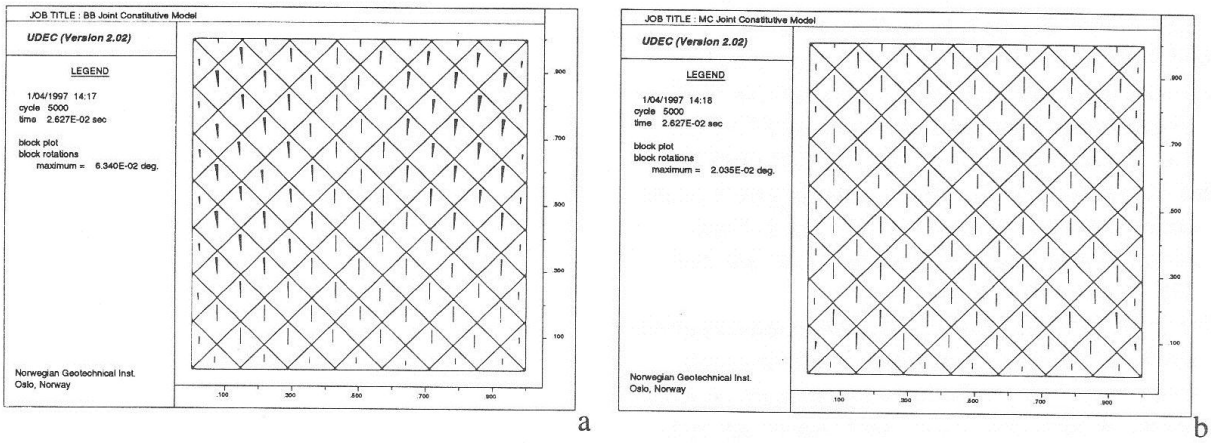

Figure 10 A comparison of block rotations (shown through rotation arcs) when using the BB model (a) and the MC model (b)

CONCLUSION

In this paper the effect of joint constitutive laws on the stress-strain behaviour of a rock mass was examined using the numerical code UDEC. The results have shown that the peak shear strength of a rock mass depends on the constitutive law used. In this respect it is revealed that the Mohr-Coulomb model, in which the dilation angle is constant, is relatively insensitive to the effect of different block sizes on the peak shear strength of a rock mass.

The BB model, which allows the modelling of variable dilation accompanying shear, predicts results similar to those from earlier physical model tests on a rock model material. These results indicate that the size of the individual blocks controls both the shear strength of the rock mass and its deformational characteristics. A closely jointed rock mass in which block rotations occur exhibits a lower stiffness but a higher peak shear strength than a rock mass with widely spaced joints.

REFERENCES

Barton, N., and Choubey, V., 1977. The Shear Strength of Rock Joints in Theory and Practice. *Rock Mechanics,* No. 1 / 2, pp. 1-54, Springer, Vienna, 1977.

Barton, N. and Hansteen, H., 1979. Very Large Span Openings at Shallow Depth: Deformation Magnitudes from Jointed Models and F.E. Analysis, *Proc. 4th Rapid Excavation and tunnelling Conference,* pp. 1331-1353, Atlanta, USA

Bandis, S.C., Lumsden, A.C., and Barton, N., 1981. Fundamentals of Rock Joint Behaviour. *Int. J. Rock Mech. Min. Sci. & Geomech. Abstr.* Vol. 20, No. 6, pp. 249-268 (1981)

Barton, N., 1982 Modelling Rock Joint Behaviour from Insitu Block Tests: Implications for Nuclear Waste Repository Design, ONWI-308, prepared by Terra Tek, Inc. *for Office of Nuclear Waste Isolation, Columbus, OH, USA.*

Barton, N. and Bandis, S., 1982. Effects of Block Size on the Shear Behaviour of Jointed Rock, Keynote Lecture, *Proc. 23rd U.S. Symposium on Rock Mechanics,* pp. 739-760, Berkeley, California (1982)

Barton, N., 1990. Scale Effects or Sampling Bias? *Proc. Int. Workshop on Scale Effects in Rock Masses,* pp. 31-55, Loen, Norway, 1990

Barton, N., and Bandis, S., 1990. Review of Predictive Capabilities of JRC-JCS Model in Engineering Practice. *Proc. Int. Symp. on Rock Joints, Loen, Norway, 1990,* pp. 603-610

Bhasin, R. and Høeg, K., 1997. Numerical modelling of block size effects and influence of joint properties in multiply jointed rock. *Submitted to Tunnelling and Underground Space Technology*

Cundall P. A., 1980 A generalised distinct element program for modelling jointed rock. Report PCAR-1-80, Contract DAJA37-79-C-0548, European Research Office, U.S. Army, Peter Cundall Associates

Cundall P.A. and Hart R.D., 1984 Analysis of block test No. 1 in elastic rock mass behavior: phase 2 - a generalization of joint behaviour. *Itasca Consulting Group,* Rockwell Hanford Operations,

Subcontract SA-957, Final Report (1984)
Cundall P. A. and Hart R.D., 1993 Numerical modeling of discontinua. *Comprehensive Rock Engineering, Principles, Practice and Projects, Vol. 2 (Ed. J.A. Hudson)*, pp. 231-243 (1993)
Saeb S. and Amadei B., 1992 Modelling rock joints under shear and normal loading. *Int. J. Rock Mech. & Min. Sci. & Geomech. Abstr.* 29, 267-278
Souley M. and Homand F., 1995 An extension of the Saeb and Amadei constitutive model for rock joints to include cyclic loading paths. *Int. J. Rock Mech. & Min. Sci. & Geomech. Abstr.* 32, 101-109